Spin-state effect on the efficiency of a post-synthetic modification reaction on a spin crossover complex

Alejandro Enríquez-Cabrera, Yongjian Lai, Lionel Salmon, Lucie Routaboul, Azzedine Bousseksou

communications chemistry

Article

https://doi.org/10.1038/s42004-025-01425-1

Spin-state effect on the efficiency of a post-synthetic modification reaction on a spin crossover complex

Alejandro Enríquez-Cabrera, Yongjian Lai, Lionel Salmon ✉, Lucie Routaboul ✉ & Azzedine Bousseksou ✉

The spin state of a metal center significantly influences the catalytic activity of its complex, a phenomenon so crucial that it has led to the dedicated field of spin catalysis. Here we investigate the effect of the spin state of an iron-based metal complex on the organic reactivity of its ligands. Specifically, we examined the post-synthetic modification of the spin crossover (SCO) complex $[Fe(NH_2trz)_3](NO_3)_2$ with *p*-anisaldehyde. A series of experiments were performed to study the transformation of the amino groups depending on the spin state of the metal. Owing to the wide thermal hysteresis loop of the SCO complex, both spin states were compared under identical conditions. The results revealed that the high-spin state led to the formation of 1.34 times more imine functional groups than the low-spin state, we propose that this arises from the different interactions between the solvent and the SCO at the different spin states.

In the past few years, there has been increasing interest in spin crossover (SCO) materials due to their versatility and ability to reversibly switch between the high-spin (HS) and low-spin (LS) states as well as their possible bistability at approximately room temperature[1–12]. This contributed to the large-scale study of the physical properties of these materials and their incorporation into different devices[13] for applications in photonics[14], electronics[15], sensors[16,17], and, more recently, in mechanics[18]. The spin state could also influence the chemical reactivity of the complex. The effect of the spin state is a subject of great interest to various scientific communities, including those in the following areas: biochemistry, catalysis, coordination, inorganic, organometallic, organic, theoretical, and analytical chemistry[19–25]. Indeed, it is well known in chemistry that the spin state of transition metal complexes[26,27] and the active sites of enzymes[28] strongly impact their chemical reactivity. In most cases, a change in the spin state during the course of the reaction is the key step in determining high selectivity and, in some cases, even if the reaction proceeds[29]. This is, for example, the case in biological oxidations such as those occurring in cytochrome P450[30,31] and superoxide reductase[32] or superoxide dismutase[33], among other enzymatic reactions[34,35].

Spin catalysis is so important that it constitutes a field of catalysis in itself, the term "spin catalysis" was introduced independently and nearly at the same time by Buchachenko[36,37] and Minaev[38] and coworkers. Examples of the effect of the spin state in catalysis reactions include β-hydride elimination[39,40], where acceleration of the reaction occurs for Fe(II) and Co(II) in the HS state; Nakamura's C–C cross-coupling reaction[41], for which, depending on the spin state of the complex, the mechanism proceeds either through stepwise Fe(II)/Fe(III) arylation (quartet spin state) or concerted out-of-sphere arylation (sextet spin state); and other iron-mediated C–H activation reactions, which have shown that a spin crossover mechanism is necessary during the catalytic cycle to promote C–H cleavage[42]. A similar situation has been observed for Fe(II)-catalyzed alkene isomerizations[43,44], alkene-diene cycloadditions[45,46], alkyne[47], and allylic[48] hydrosilylations. It is important to mention that in all these cases, the starting metallic complex is not the active species. Indeed, during the course of the reaction, the coordination and spin states of the metal change in the reaction medium, leading to the active catalyst. Finally, when the spin state effect is exploited, better catalytic properties can be obtained[49], leading, for example, to improved electrocatalytic efficiencies[50–54]. Other authors have demonstrated the strong influence of the spin state of the metallic center on the chemical reactivity of metallic[55–59] and covalent organic frameworks[60] (MOF and COF, respectively) or in polyoxometalates[61]. However, in most of these cases, the spin state of the metallic center is changed either by mechanical exfoliation[62] or oxidation[60] of the metallic center, or by a host-guest interaction[63–65], making reversible switching between the two spin states impossible.

Recently, Umeyama et al. showed that the spin state of their spin crossover material has a significant impact on the quantity of defects in these compounds. Specifically, when the considered clathrate is suspended in methanol, the solvent substitutes some pyrazole ligands coordinated to the iron atom, thereby introducing defects into the material[66].

CNRS, Laboratoire de Chimie de Coordination, Toulouse Cedex 4, France. ✉e-mail: lionel.salmon@lcc-toulouse.fr; lucie.routaboul@lcc-toulouse.fr; azzedine.bousseksou@lcc-toulouse.fr

The term 'post-synthetic modification" was introduced for the first time in 2007[67] in the field of MOF as an analogy to protein post-translational modification (PTM)[68]. However, only a few studies have been done regarding the post-synthetic modification (PSM) method in this 1D polymeric triazole SCO complexes[55,69–74]. In the last couple of years, our research team has focused on developing and understanding a PSM method involving SCO coordination polymers, such as $[Fe(NH_2trz)_3](NO_3)_2$ (complex **1**)[69,73,74].

We have demonstrated that a complete solid-liquid PSM is achievable and that the efficiency of this method is temperature-dependent. The observed increase in efficiency with rising temperature can be attributed to one or a combination of the following factors:

Thermodynamic activation

Increasing the temperature provides the necessary energy to overcome the activation barrier for the formation of the functional group, facilitating the synthesis of the target product. When a product is not obtained or when the reaction rate is slow, the typical strategy is to increase the reaction temperature.

Temperature-induced changes in reactant-solvent interactions

Increasing the temperature could also affect the interactions between reactants or between a reactant and the reaction solvent, altering their behavior and enhancing the reactivity of the system. Notably complex **1** is insoluble in the reaction solvent (ethanol) and it exhibits a very compact molecular arrangement due to strong interactions between the polymer chains, which lack pores. Our previous work has demonstrated the central role of ethanol in the PSM process; where ethanol interacts with the polymer chains, promoting their separation and thus enhancing the reactivity of the amino functional group on the ligand[74].

Spin-state effects

The spin state of complex **1** may also impact the efficiency of the PSM process. The reactivity of the iron complex could be influenced by its spin state through electronic and/or steric factors; the latter being linked to the change in volume that occurs during the spin transition[13–54].

In the field of switchable materials based on spin crossover complexes, we are particularly interested in the effect of the spin state. Several studies have explored the spin-state dependence of the reactivity of Fe(II) complexes[64,75–78]. However, in these reports, the spin states of the different complexes studied were modified by changing either the ligand or anion or by incorporating a guest molecule in the crystalline lattice. Such modifications inherently complicate the interpretation of results, as they do not allow for the independent study of both spin states under identical conditions for the same complex. As a result, it remains challenging to fully isolate the effect of the spin state from other experimental variables.

In contrast, the parent complex in our study exhibits a pronounced thermal hysteresis above room temperature, providing a significant advantage: it allows for the investigation of both spin states under identical experimental conditions, particularly at the same temperature. This feature enables us to more effectively differentiate between the effects of the spin state and other potentially confounding factors.

In this manuscript, we demonstrate that the transformation of the amino group present on the iron-coordinated ligand is influenced by the spin state of the metal. To the best of our knowledge, this is the first report of such an effect. While previous studies have shown that the spin state affects the reactivity of the metal center, our findings reveal that the spin state also modulates the reactivity of a ligand substituent, even though this substituent is not directly coordinated to the metal. This result suggests that the spin transition affects not only the reactivity at the metal center but also influences the reactivity of the entire complex.

Results and discussion

Various experiments were conducted to assess the contribution of each identified factor (thermal activation, structural effect, spin state effect) to the enhanced effectiveness of the PSM method. For this study, we used our model reaction: the formation of an imine functional group by the action of *p*-anisaldehyde on complex **1** (batch 1)[74]. The efficiency of the PSM method leading to complex **2** increased drastically when the reaction was carried out at 90 °C. As shown in Fig. 1b, the PSM reaction was completed in just 1 h at 90 °C whereas it took 72 h at 35 °C.

To determine whether this improvement is mainly due to the activation energy barrier being overcome, we also tested the effect of temperature on the reaction between 4-amino-1,2,4-triazole and *p*-anisaldehyde, which forms the corresponding ligand. Although the aminotriazole ligand is fully soluble and the SCO complex is insoluble, this reaction provides a straightforward model to assess whether a similar temperature effect occurs with the free ligand. If observed, this effect could be attributed to overcoming the thermal energy barrier. Before discussing the results, it is important to mention that the yields were obtained from ^{1}H-NMR in the presence of an internal standard. For the ligands, we directly sampled the reaction medium, and for the complex, we performed the digestion method. The process known as digestion consists of the decoordination of triazole ligands from iron, enabling the quantification of the proportion of aminotriazole and imine ligands in the complex. The complex is then digested under aqueous basic conditions in the presence of chloroform, followed by the separation of the organic and aqueous phases, with the imine ligand in the organic phase and aminotriazole in the aqueous phase (for further details, see ESI S3)[69].

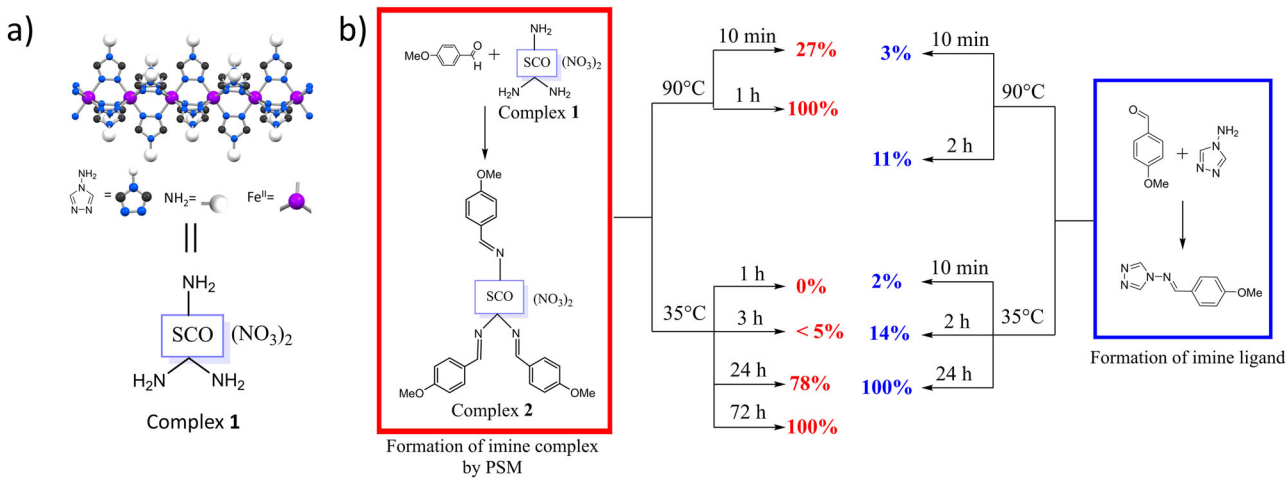

Fig. 1 | Overview of the chemical structure of the SCO complex and the experimental conditions to obtain the imine (for the ligand and the complex). a 1D polymeric structure of $[Fe(NH_2trz)_3](NO_3)_2$; **b** Experimental conditions and yields for the synthesis of the ligand (imine) and complex **2**.

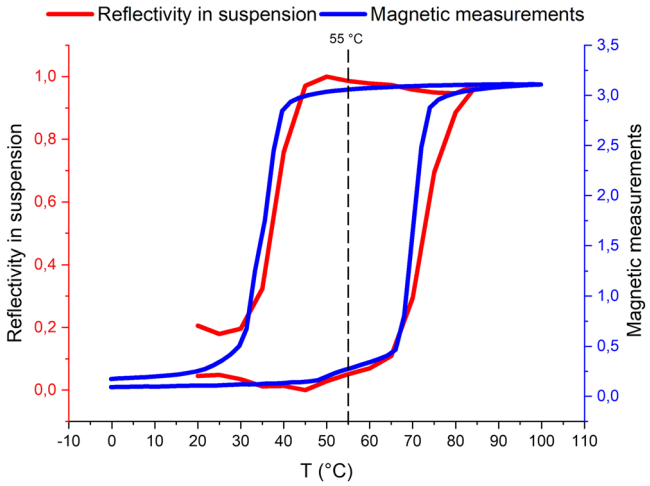

Fig. 2 | Comparison of the SCO properties in suspension and in the solid state. Variable temperature magnetic susceptibility for the solid (blue curve) and optical reflectivity in an ethanol suspension (red curve) for complex **1**.

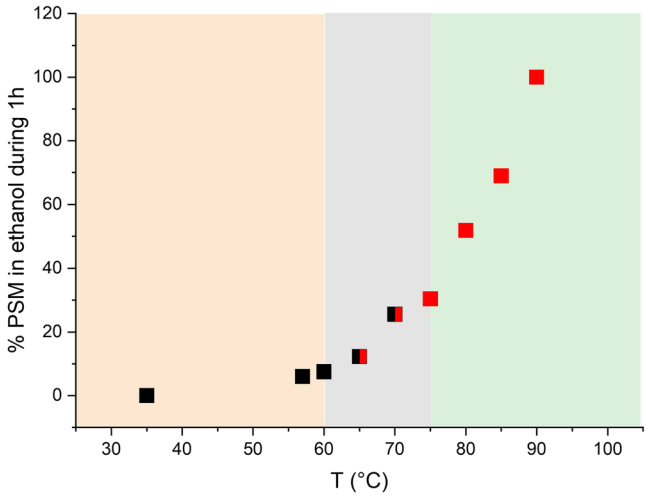

Fig. 3 | Overview of the PSM yields as a function of the temperature for one hour of reaction. Yields of the PSM reaction at different temperatures, in the low-spin state region (black squares), intermediate spin state region (black and red squares), and the high-spin state region (red squares).

Interestingly, temperature had little impact on the yield of the imine ligand. After 2 h of reaction, the yields were 11% at 90 °C and 14% at 35 °C (Fig. 1b). These results suggest that the pronounced temperature dependence is specific to the PSM reaction on complex **1** and cannot be attributed solely to thermal activation. Given that the kinetics of imine formation differ between the ligand and the complex, we decided to investigate this further using batch 1 of complex **1**. The PSM reaction was performed for 1 h across a temperature range of 35 °C–90 °C to evaluate whether the efficiency increased linearly and to identify the temperature at which the most significant change occurred.

Before discussing these results, it is important to first outline the spin crossover properties of complex **1**. The SCO properties of complex **1** were determined by measuring the magnetic susceptibility at a variable temperature (blue curve, Fig. 2). The temperatures of the LS-to-HS and HS-to-LS transitions are 70 °C and 36 °C, respectively, with a width of the hysteresis loop of 34 °C, in agreement with previous studies[69,73,74]. Another effective method for monitoring the spin crossover is the measurement of the optical reflectivity at a variable temperature, which takes advantage of the color change between the two spin states. The optical reflectivity was also measured as a function of the temperature for the complex **1** suspended in ethanol (red curve in Fig. 2). This is particularly relevant since the magnetic susceptibility of pure complex **1** was measured in the solid state, while the PSM reaction occurs in the presence of ethanol. Although complex **1** is not soluble in ethanol, the solvent may significantly influence the molecular arrangement and, consequently, the SCO properties[74]. Nevertheless, the transition temperatures measured in suspension ($T_{1/2}\uparrow = 72.5$ °C, $T_{1/2}\downarrow = 37.5$ °C, $\Delta T = 35$ °C) are in close agreement with those observed for the pure complex **1** in the solid state for the first cycle. In contrast to those in the solid state, in suspension, all the following thermal cycles remain similar to the first cycle, certainly due to the presence of trapped solvent molecules (see ESI S1.A). Importantly, the abrupt spin transition and the hysteresis loop are preserved even if complex **1** is suspended in ethanol.

The yields of the PSM reaction after one hour are indicated in Fig. 3 as a function of the temperature. It is important to note that the reaction was carried out in a hermetically sealed pressure tube, which allows heating to 90 °C and thus beyond the boiling temperature of ethanol.

The results shown in Fig. 3 support the hypothesis that the spin state affects the efficiency of the PSM reaction. We can distinguish three distinct temperature regions based on the reaction progress. The first region corresponds to the low-spin (LS) state (between 35 and 60 °C), where imine formation is minimal. In the second region, the yield increases slightly, from approximately 7% at 60 °C to 30% at 75 °C. In the third region, a significant increase in yield is observed, from 30% at 75 °C to 100% at 90 °C. This behavior suggests that the PSM reaction becomes more efficient starting from the spin transition, where both spin states coexist, and reaches its highest efficiency when complex **1** is exclusively in the high-spin (HS) state. These results seem to indicate that complex **1** is more reactive in the HS state than in the LS state. However, temperature is a critical factor influencing reaction efficiency. It is well known that the diffusion of solvents and reagents in certain materials is temperature-dependent[79–85]. In the absence of direct evidence suggesting that the diffusion of ethanol and reactants within the particles of complex **1** remains constant across the studied temperature range, this factor should not be overlooked. As in heterogeneous catalysis, the reaction yield involving a solid reactant can be significantly influenced by the quality of contact between reactants. Furthermore, three of the four PSM reactions performed with complex **1** in the HS state were solvothermal syntheses (reactions carried out in sealed systems at temperatures above the solvent boiling point)[86–88]. Such types of reactions often yield results distinct from those conducted below the boiling point, due in part to substantial changes in the physical properties of the solvent. Given these variables, further studies are necessary to isolate the specific effect of the spin state from other influencing factors.

It is crucial to compare the yields of the PSM reactions as a function of the spin state of complex **1** at the same temperature. To this end, we took advantage of the thermal hysteresis loop observed for complex **1** in suspension, which covers a range of temperatures at which both spin states can be stabilized at specific temperatures. The temperature chosen for this study was 55 °C, corresponding to the temperature in the middle of the hysteresis loop (indicated by a dashed line in Fig. 2).

The suspensions of complex **1** in different spin states were systematically prepared from the same batch of complex **1**. For the low-spin (LS) state, 50 mg of complex **1** was suspended in 2 mL of ethanol and placed in an oil bath at 55 °C. The high-spin (HS) state was obtained by heating a similar suspension to 90 °C for 2 min, which was confirmed by a color change of the complex **1** particles to white. The suspension was then quickly transferred to the 55 °C bath, where the particles remained white, indicating that the complex stayed in the HS state.

It should be noted that heating to 90 °C to stabilize the HS state could also cause an irreversible modification of the molecular arrangement between the polymer chains. Therefore, a comparative sample, designated LS2, was prepared: complex **1** was heated to 90 °C for 2 min, then cooled to room temperature for 5 min to allow the complex to return to the low-spin state, before being placed in an oil bath at 55 °C. After maintaining all three samples at 55 °C for 10 min, the aldehyde (previously heated to 55 °C) was

a)

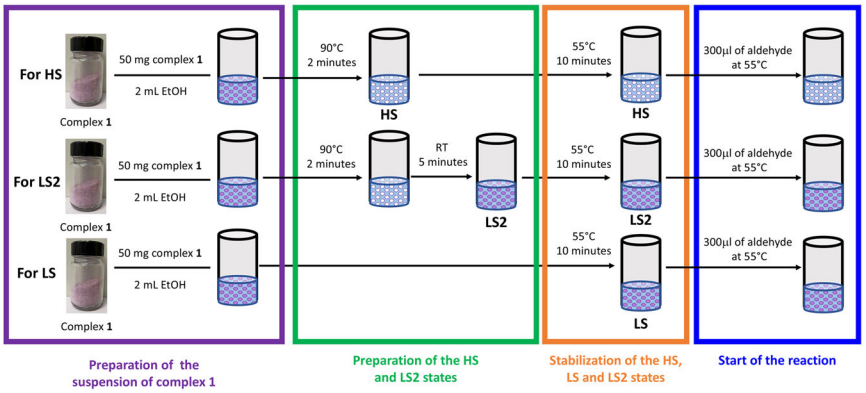

b)

	time (hour)	1	3	4
PSM as function of the spin state(%)	LS	6	29	50
	HS	8	41	72
	LS2	/	33	51
difference in the efficiency of the PSM (%)	D_{HS-LS2}	/	8	21
	D_{HS-LS}	2	12	22
	D_{LS2-LS}	/	4	1

Fig. 4 | General procedure for the PSM reaction at different spin states. a Scheme of the procedure used to prepare complex **1** in the HS, LS, and LS2 states; **b** Table of the yields of the PSMs depending on the reaction time and the spin state of complex **1** (batch 1).

added to the three suspensions, initiating the reaction (the experimental steps are shown in Fig. 4a). Thus, all reactions between the aldehyde and the iron complex were carried out under identical conditions for the three samples (see ESI S2.A).

First, regardless of the spin state of the complex, a drastic increase in the efficiency of the PSM method was observed after 4 h of reaction, as previously reported (Fig. 4b)[74]. Indeed, we had previously noted that when the PSM yield reaches 30–40%, the reactivity increases significantly. This phenomenon was attributed to the introduction of imine groups, which promote better separation of the polymer chains in the complex, thereby facilitating the PSM reaction. For a reaction time of 4 h, the PSM yield of complex **1** in the HS state is significantly greater than for the LS and LS2 states. Thus, this result suggests that the PSM reaction occurs more rapidly in the HS state than in the LS state. The higher reaction rate in the HS state could be explained by electronic and/or steric factors. On one hand, the electron density at the NH_2 functional site is influenced by the spin state of the iron complex: The more nucleophilic the nitrogen, the faster the reaction with the aldehyde. On the other hand, the speed of reactions involving a solid compound depends strongly on the ease and speed with which the two reactants come into contact. It is well known that a spin transition from LS to HS leads to an increase of the molecular volume of the SCO complex. Concerning 1D "Fe-triazole" SCO polymers and according to the work of Grosjean et al.[89–92], the distance between iron atoms in neighboring polymer chains is generally greater in the HS state than in the LS state. This greater interatomic distance could facilitate the reaction between the amino and aldehyde functionalities. However, they also found that complex **1** is unique since it does not follow the generally high global volumetric expansion observed in this family of SCO complexes. Upon transitioning from the LS to the HS state, the Fe-N bond elongates, and the polymer chain axis expands, but there is a concomitant contraction in all other directions[92,93]. As a result, the total volumetric expansion is only about 1%, which is significantly smaller than the expansions observed in other complexes of this family (6% for $[Fe(NH_2trz)_3](BF_4)(SiF_6)_{0.5}$[94], 10% for $[Fe(Htrz)_2(trz)](BF_4)$[89] and 5% for $[Fe(NH_2trz)_3]SO_4$[95]). Therefore, this volumetric change may not be sufficient to explain the increase in the PSM yield. Moreover, when the experiments were performed in toluene instead of ethanol, no reaction occurred even if the complex was in the HS state[69,74]. This indicates that, while the general volumetric expansion cannot be entirely ruled out, the solvent plays a critical role in the PSM reaction. It is also plausible that the strength and number of interactions between the polymeric chains and ethanol depend on the spin state of the iron complex. As we have previously suggested[74], stronger interactions between the complex and ethanol could lead to a greater separation of the polymer chains, thus promoting a faster PSM reaction. Additionally, the yields of PSM products from the LS2 complex were slightly greater than those from the LS complex. A possible explanation for this is that the molecular arrangement of the LS2 complex differs from that of the LS complex. Indeed, heating the suspension of the complex in ethanol to 90 °C may enhance the interactions between the solvent and the polymeric chains of the iron complex resulting in a new molecular arrangement of the material. Thus, the reactivity of the amino group on the aldehyde appears to be influenced by the spin state of the iron.

We then sought to assess the reproducibility of these promising results. For this study, we focused mainly on the reactivity of complex **1** in the HS and LS2 states. To do so, we tested 4 new batches of complex **1** (Batches 2–5) and conducted a total of forty-four experimental sets. Each set consisted of parallel reactions, one with complex **1** in the HS state and one in the LS2 state, all under the same experimental conditions. Indeed both reactions were performed simultaneously, in the same oil bath at 55 °C, with identical reaction times, and using the same quantities of solvent and reagent (the same bottles of ethanol and aldehyde). After the work-up, 2 samples from each spin-state experiment were taken and independently treated by the digestion method. To validate our digestion method (which involves digestion of the complex and subsequent quantification by NMR; for more details, see ESI S3 pages 19–20), we prepared several physical mixtures containing known quantities of the pure imine and amine complexes. These mixtures underwent the same procedure as the PSM reaction complexes including grinding, sampling, digestion, and NMR analysis of the two phases. This validation study demonstrated that the digestion method we developed to quantify the imine formed in the complex is accurate, precise, and reproducible. In general, the values obtained correspond to the expected value of the imine percentage, with an error that is usually not larger than ±2% (for more details, see ESI S3.D pages 20–26).

With these 44 sets of experiments, we evaluated the effects of various parameters on the efficiency of the PSM reaction: only the effect of spin state (Batch 2, S4.A and Batch, 4 S4.D in ESI), reaction time (Batch 2, S4.B and Batch 5, S4.F in ESI) presence of a low percentage of water in the reaction medium (Batch 3, S4.C in ESI), and sonicating prior the reaction (Batch 3, S4.C and Batch 4, S4.E in ESI). To ensure the reliability and reproducibility of our results, several additional sets of experiments (up to 10 sets) were conducted under identical conditions.

This study systematically demonstrated that the percentage of imines was higher when complex **1** was in the HS state compared to the LS2 state. While a full discussion of the reproducibility can be found in the ESI (S4, pages 26–71), the impact of reaction time on the efficiency of the PSM method for batch 5 of complex **1** is illustrated in Fig. 5 (see ESI S4.F).

In all the cases, the percentage of imines was greater when the complex was in the HS state than in the LS2 state. This difference in reactivity is significant enough to clearly distinguish between experiments using the complex in the HS state and those in the LS2 state. As shown in Fig. 4, when the percentage of imines formed from the HS state is between 40 and 50% (set 1–4, reaction time <5 h), the reactivity in the LS2 state is approximatively 10% lower than in the HS state. When the percentage of PSM from the HS state is between 70 and 90% (set 5–18, reaction time >5 h), the gap increases to 20%. Apart from experiment set 7 (which is one of two sets

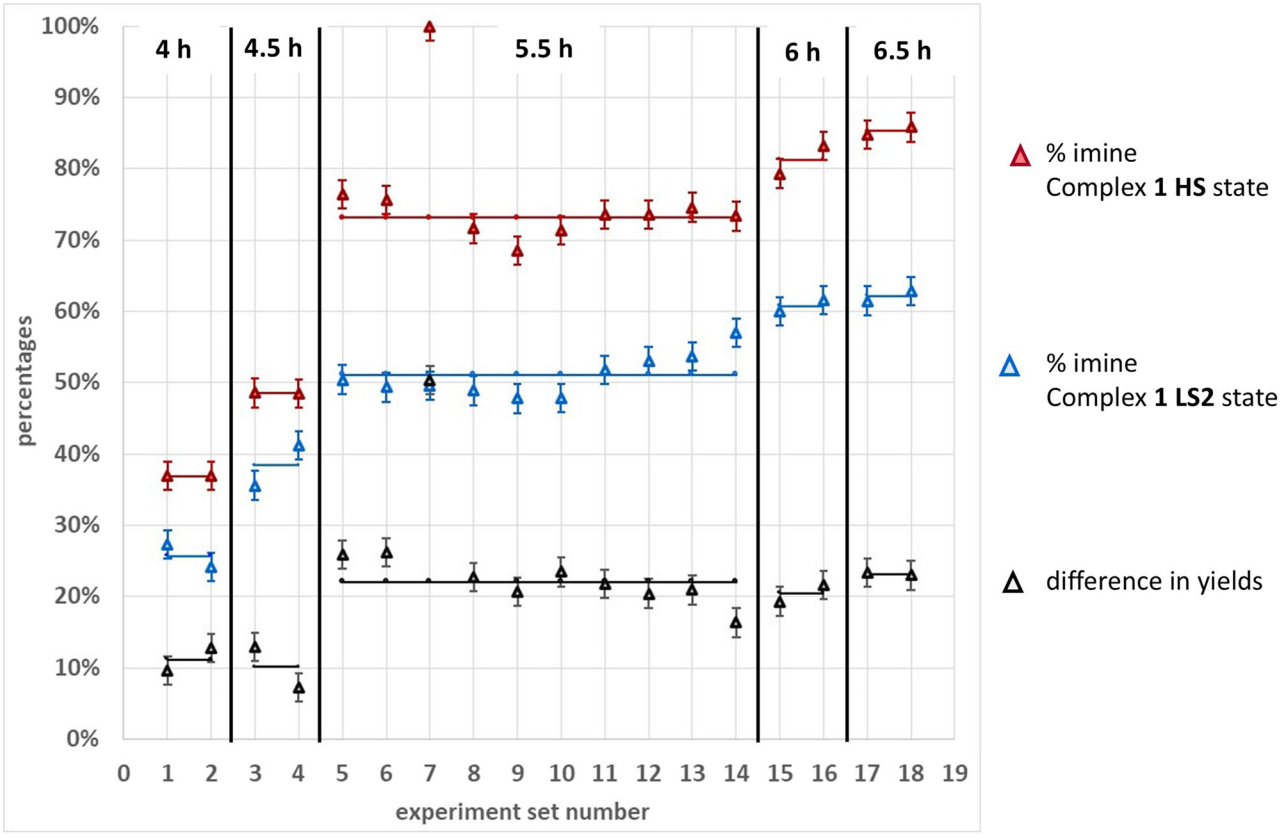

Reaction time (h)	4	4.5	5.5	6	6.5
average % imine complex **1 HS**	37.0	48.5	73.2	81.3	85.3
average % imine complex **1 LS2**	25.7	38.4	51.1	60.8	62.1
average % difference in yield	11.2	10.1	22.1	20.5	23.2

Fig. 5 | Results of the PSM at different spin states for batch 5 of the complex 1. Yields of imine obtained for batch 5 in the HS and LS2 state after 4, 4.5, 5.5, 6, and 6.5 h of reaction.

considered aberrant in the entire study), all the other results are consistent. The findings for batches 1 and 5 of complex **1** also align well. In particular, the results obtained from batch 5 confirm that the differences in imines percentages between the two spin states can reach 20%. However, in the case of batch 5, a reaction time of 5.5 h (Fig. 5) is needed to achieve a yield of 70% (for complex **1** in the HS state), whereas, for batch 1, only 4 h is sufficient (Fig. 4b).

This variation in reaction time can be attributed to two main factors: (1) the difference in the amount of water (traces amounts or very small quantities) present in complex **1** and/or in ethanol and (2) the variation in the size of the SCO particles and/or their agglomerates. We have previously shown that the presence of even a small quantity of water accelerates the PSM reaction[74]. Furthermore, if, as we have shown in earlier work[74], the PSM reaction likely occurs between complex **1** in the solid state and the aldehyde in the solution. Therefore, the size of the SCO particles, as well as the degree of particle agglomeration, is expected to significantly influence the reaction time. Specifically, smaller particles have a larger surface area, which facilitates more efficient contact with the aldehyde and thus leads to shorter reaction times. To test this hypothesis, we conducted additional experiments in which complex **1** in suspension in absolute ethanol was subjected to sonication prior to the reaction steps outlined in Fig. 4a, and later on ethanol 96% was added so that the reaction was carried out in 98% ethanol rather than absolute ethanol. As anticipated, these modifications allowed for the achievement of a 70% yield in batch 5 (HS state), within 4 h as opposed to 5.5 h under the original conditions (see ESI, pages 6, 38–45). Under these revised experimental conditions, the difference in yields between the two spin states of complex **1** is approximately 15%.

For the 42 experimental sets (excluding two aberrant sets), we calculated: (1) the ratio of HS to LS2 based on the percentage of imine formed (see ESI S5.A) and (2) the ratio of the difference in the yields between the two spin states relative to the yield obtained in the HS state (see ESI S5.B). On average, 1.34 times more imine is formed when the complex is in the HS state compared to the LS2 state (Fig. 6). These results are consistent across experiments (see also the standard deviation analysis on the ESI S5.C), reinforcing the conclusion that the spin state of the metal has a significant impact on the reactivity of the complex.

The effect of suspension dilution on the reactivity difference between the two spin states of the complex was investigated. Increasing the volume of ethanol could improve the dispersion of complex **1** particles, potentially leading to shorter reaction times. This is because reducing the size of the particles or aggregates increases the surface area, thereby accelerating the reaction. However, in order to keep the number of aldehyde equivalents

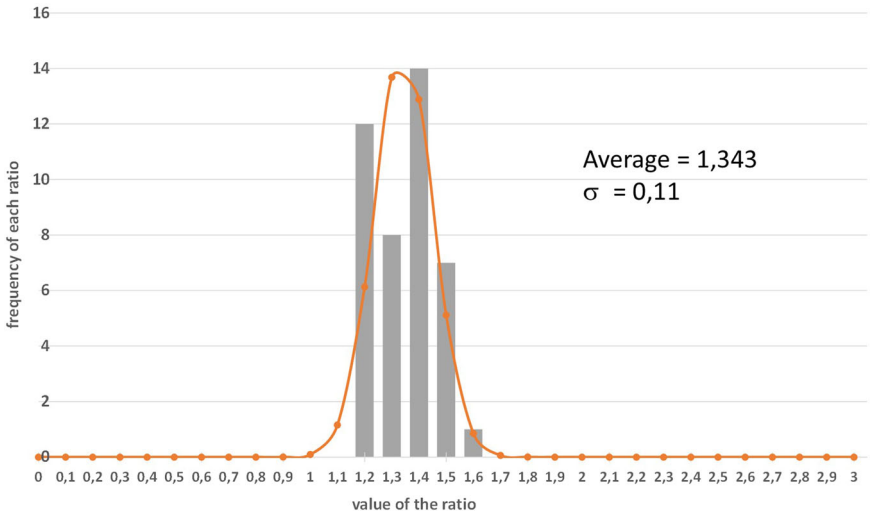

Fig. 6 | Distribution of the ratio %HS/%LS for all experiments performed. The frequency of the ratio of %HS/%LS2 for 42 samples.

relative to complex **1** constant, the amount of aldehyde must remain unchanged. Therefore, adding ethanol reduces the aldehyde concentration, which may slow down the reaction. Reactions were performed with complex **1** from batch 6, using 2 mL (standard volume), 6 mL, and 10 mL of ethanol. This preliminary study (Batch 6, S4.G in ESI) shows that increasing the ethanol volume slows the reaction, suggesting that the dilution of aldehyde is the limiting factor. To achieve a significant reactivity difference between the spin states, the imine formation from the PSM reaction with complex **1** in the HS state must exceed 60%. As a result, reaction times were adjusted according to the ethanol volume: 5.5 h for 2 mL, 8 h for 6 mL, and 10 h for 10 mL. As shown in Fig. 7, increasing the ethanol volume by a factor of three or five has a limited effect on the reactivity difference between the two spin states. A difference of about 20% in imine formation is observed between reactions conducted with complex **1** in the HS state and those carried out with the LS2 state. These results confirm that complex **1** in the HS state is more reactive toward aldehyde than in the LS2 state.

The kinetics of the PSM depend on the spin state of complex **1**, but do the properties of the synthesized materials also depend on the spin state of the parent complex? Fully transformed complexes **2**, obtained in ethanol at different temperatures (1 h at 90 °C and 72 h at 35 °C) were characterized by powder X-ray diffraction and variable temperature magnetic susceptibility measurements. Regardless of the temperature used to obtain complex **2**, the observed crystalline features are strikingly similar (Fig. 8), and the SCO properties remain nearly identical in both cases.

The magnetic susceptibility as a function of temperature shows a gradual evolution, with a midpoint transition ($T_{1/2}$) centered around 257 K, as previously reported[69,73,74]. This suggests that, regardless of the reaction temperature, the final complex **2**, is identical in all cases.

Conclusion

As shown in this manuscript, the temperature-dependent increase in PSM efficiency can be attributed to three main factors: (1) overcoming the activation energy barrier; (2) temperature-induced changes in solvent interactions with complex **1**; and (3) the spin state of complex **1**. However, the results from our experiments indicate that the spin state is the predominant factor. In particular, due to the significant hysteresis loop observed above room temperature for the parent SCO complex **1**, we investigated the formation of imines from both spin states under identical experimental conditions. We observed up to 23% improvement in the efficiency of the PSM when going from the LS2 to the HS state for complex **1**. Across 44 experimental sets conducted on 5 different batches of complex **1**, we consistently found that the yield of imines was greater when complex **1** was in the HS state compared to the LS2 state. The large number of experiments, coupled with an error margin of ±2% from the digestion method (±2%) confirms that the difference in reactivity between the two spin states is both significant and reproducible. On average, the imine yield was 1.34 times greater in the HS state than in the LS2 state. We hypothesize that, while electronic effects cannot be completely ruled out, the spin state has a substantial impact on the interactions between the polymeric chains of complex **1** and the solvent. In the high-spin state, complex **1** likely interacts more strongly with ethanol, promoting better separation of the polymeric chains and thereby facilitating the PSM reaction. To further explore this hypothesis, ongoing experimental and theoretical studies are being conducted, combining both modeling and empirical data, to elucidate the underlying mechanism by which the spin state affects ligand reactivity. This article provides the first example of the influence of the spin state on the post-synthetic modification of such a 1D SCO coordination polymer. More broadly, and notably, to the best of our knowledge, this is the first report in which the effect of the spin state has been shown to impact the organic reactivity of a functional group within a metal complex. Our findings highlight that the spin state effect is not confined to atoms directly coordinated to the metal, but extends to the reactivity of the entire ligand. Additionally, we found that the spin state primarily affects the kinetics of product formation, with complex **2** synthesized at 35 °C exhibiting identical structural and SCO properties to those synthesized at 90 °C. These results are of considerable significance not only for the spin crossover (SCO) community but also for the broader field of chemistry. By enhancing the reactivity of one spin state of the complex and employing the PSM method, a larger variety of complexes can be synthesized from a single parent material, offering the potential to fine-tune material properties for specific applications. This is an important issue in materials science since it is possible to fine-tune the property for each application. Moreover, the PSM of the more active spin state complex followed by a decoordination reaction (digestion method) may lead to the formation of a wide range of novel organic molecules. The coordination of organic molecules to the metal modifies their reactivity, facilitating the synthesis of compounds that might otherwise be difficult or impossible to obtain. The spin-state effects of SCO complexes on catalysis and molecular recognition are currently under investigation.

Methods

In this section, are only described the general methodologies used in this manuscript, for a detailed procedure concerning all the different experiments done, it is necessary to read the supplementary information.

Synthesis of $[Fe(NH_2trz)_3](NO_3)_2$ (1)

A total of 2.62 g (10 mmol) of $Ba(NO_3)_2$ and 100 mg of ascorbic acid were dissolved in 20 mL of distilled water. In a separate flask, 2.78 g (10 mmol) of $FeSO_4{\cdot}7H_2O$ was dissolved in 10 mL of distilled water. Both solutions were heated slowly until the reagents were completely dissolved. Then, the

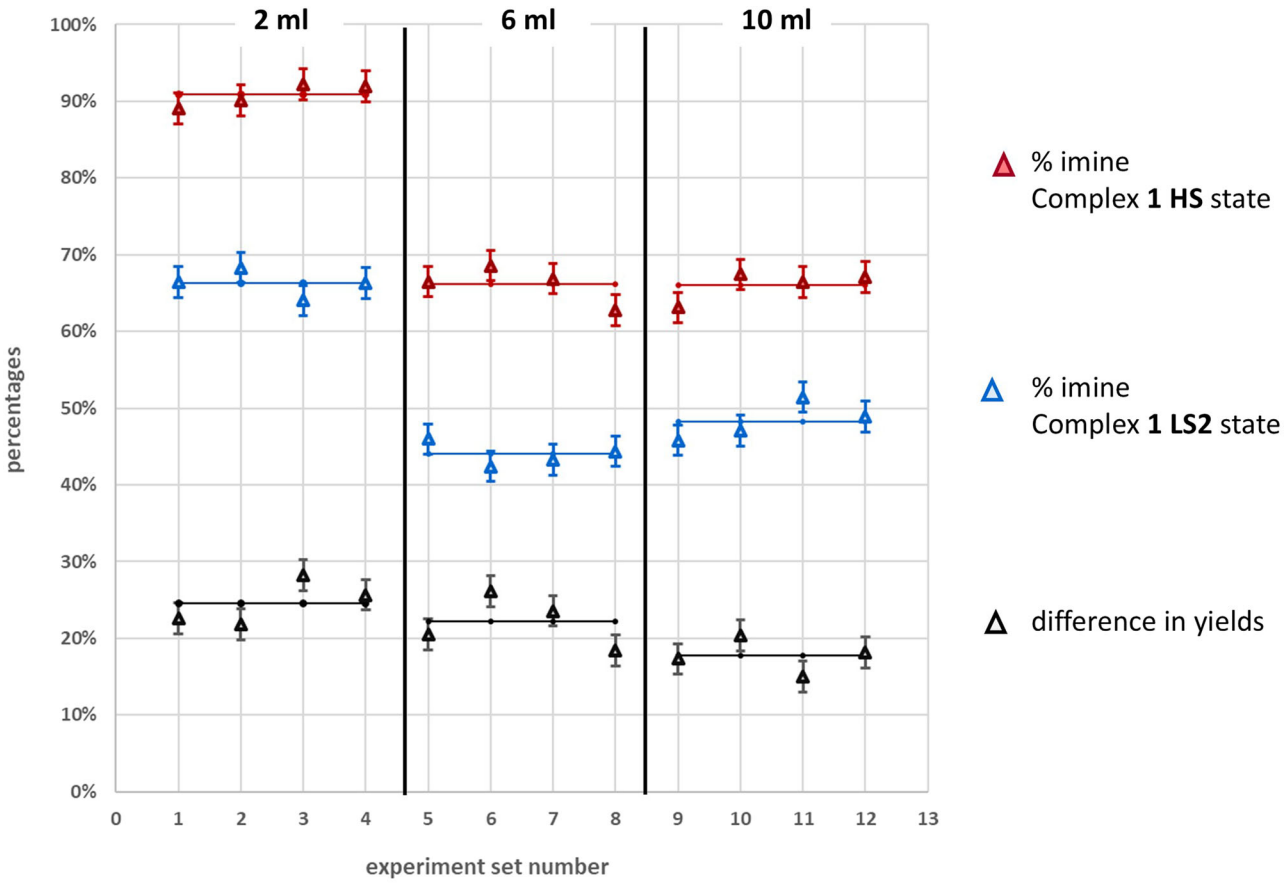

ml of ethanol	2	6	10
average % imine complex **1 HS**	90.8	66.2	66.0
average % imine complex **1 LS2**	66.3	44.0	48.3
average % difference in yield	24.6	22.2	17.7

Fig. 7 | Results of the PSM at different spin states and volumes of ethanol. Yields of imine obtained with different ethanol volumes in the reaction.

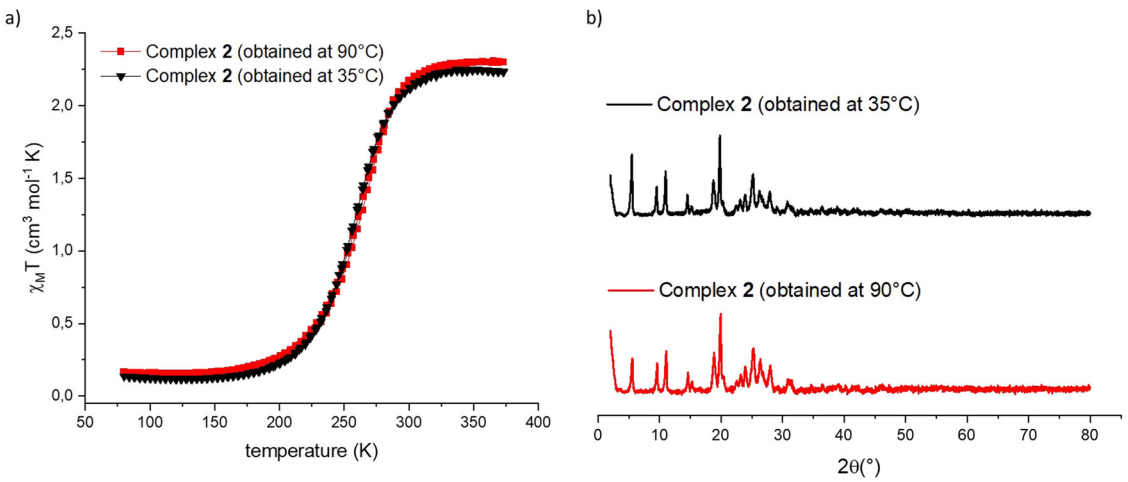

Fig. 8 | Magnetic and PXRD measurements of the imine complex. a Variable temperature magnetic susceptibility measurements and **b** diffractogram of PXRD measured at room temperature for complex **2** obtained in ethanol at 35 °C (LS state, black) and 90 °C (HS state, red).

solution containing the iron was added to the solution of barium nitrate, which resulted in the immediate precipitation of barium sulfate. The suspension was left to cool to room temperature and then centrifuged, resulting in 30 mL of a 0.333 M solution of $Fe(NO_3)_2$.

First, 2.52 g (30 mmol) of 4-amino-1,2,4-triazole was dissolved in 10 mL of ethanol, and then, 30 mL of a freshly prepared 0.333 M solution of $Fe(NO_3)_2$ was added to it under vigorous stirring; the mixture was stirred for 3 h, resulting in a pink slurry. The mixture was centrifuged and washed 3 times with 20 mL of ethanol and then 3 times with 20 mL of diethyl ether, after which it was dried in an oven at 60 °C, resulting in 2.76 g (65%) of the product.

Methodology for the post-synthetic modification (general procedure)

50 mg of SCO complex **1** was suspended in 2 mL of absolute ethanol in a vial. For the **LS** sample, the vial was immersed in an oil bath at 55 °C; for the **HS** sample, the vial was immersed first at 90 °C for 2 min and then immersed in the same oil bath used for the **LS** sample at 55 °C; for the **LS2** sample, the vial was immersed first at 90 °C for 2 min and then left to cool at room temperature for 5 min; and finally, it was immersed in the same oil bath used for the **LS** and **HS** samples at 55 °C. Once the three samples were in the oil bath, we waited 10 min to allow the samples to settle at 55 °C. In a separated vial, *p*-anisaldehyde was heated at 55 °C. Then, 300 µL of *p*-anisaldehyde previously heated at 55 °C was added carefully to each sample so that the spin state remained the same, and the vial was closed and stirred for a specific period of time.

At the end of the reaction, the tube was immersed immediately in an ice-water-ethanol bath to stop the reaction, and after 1 min, 0.5 mL of ethanol and 10 mL of diethyl ether were added to the mixture. The mixture was then centrifuged and washed 2 times with 10 mL of diethyl ether, after which it was left to dry overnight.

Digestion of the sample

The digestion was performed following our previously reported methodology[2,3]. A standard solution of 1,3,5-trimethylbenzene (TMB) in $CDCl_3$ and 2,2-dimethyl-1,3-propanediol (NPG) in D_2O was made for each day of analysis (to avoid evaporation of the solvent in the standard solution); this was accomplished by weighing a thoroughly known quantity of the standard (approximately 20 mg) in a 10 mL volumetric flask.

The whole PSM complex was ground to obtain a homogeneous sample. Then, approximately 20 mg of the PSM complex was thoroughly weighed, and 2 mL of D_2O, 2 mL of $CDCl_3$, and 276 mg of K_2CO_3 were added. The tube was closed and stirred vigorously and sonicated for approximately 5–10 min (until the appearance of a yellow-orange suspension with no residues of the SCO powder), and the resulting mixture was then centrifuged, allowing separation of the organic and aqueous phases and an interlayer of iron residues. Under these conditions, the complex is destroyed and allows the noncoordinated ligands to be recovered and quantified (aminotriazole in the aqueous phase and imine in the organic phase). Then, 0.4 mL of the $CDCl_3$- or D_2O-digested solution was added to an NMR tube, and 0.2 mL of the corresponding standard solution was added, after which the ^{1}H-NMR data were recorded.

Data availability

The data that supports these results are available in the supplementary materials of this article.

Received: 2 September 2024; Accepted: 22 January 2025;
Published online: 12 February 2025

References

1. Kahn, O. & Martinez, C. J. Spin-transition polymers: from molecular materials toward memory devices. *Science* **279**, 44–48 (1998).
2. Niel, V., Martinez-Agudo, J. M., Muñoz, M. C., Gaspar, A. B. & Real, J. A. Cooperative spin crossover behavior in cyanide-bridged Fe(II)-M(II) bimetallic 3D Hofmann-like networks (M = Ni, Pd, and Pt). *Inorg. Chem.* **40**, 3838–3839 (2001).
3. Zhang, Y. et al. Spin crossover iron complexes with spin transition near room temperature based on nitrogen ligands containing aromatic rings: from molecular design to functional devices. *Chem. Soc. Rev.* **53**, 8764–8789 (2024).
4. Hegazy, M. B. Z., Hassan, F. & Hu, M. Hofmann-type cyanide bridged coordination polymers for advanced functional nanomaterials. *Small* **20**, 1–36 (2024).
5. Ohtani, R. et al. Precise control and consecutive modulation of spin transition temperature using chemical migration in porous coordination polymers. *J. Am. Chem. Soc.* **133**, 8600–8605 (2011).
6. Ni, Z. P. et al. Recent advances in guest effects on spin-crossover behavior in Hofmann-type metal-organic frameworks. *Coord. Chem. Rev.* **335**, 28–43 (2017).
7. Lochenie, C. et al. Spin-crossover iron(II) coordination polymer with fluorescent properties: correlation between emission properties and spin state. *J. Am. Chem. Soc.* **140**, 700–709 (2018).
8. Brachňaková, B. et al. Spin crossover metal-organic frameworks with inserted photoactive guests: on the quest to control the spin state by photoisomerization. *Dalton Trans.* **50**, 8877–8888 (2021).
9. Ma, C. & Besson, C. Precise control of the degree and regioselectivity of functionalization in nitro- and amino-functionalized di(trispyrazolylborato)iron(ii) spin crossover complexes. *Dalton Trans.* **50**, 18077–18088 (2021).
10. Desrochers, P. J. et al. Rational design of iron spin-crossover complexes using heteroscorpionate chelates. *Inorg. Chem.* **61**, 18907–18922 (2022).
11. Šagátová, A. et al. Above room temperature spin crossover in mononuclear iron(ii) complexes featuring pyridyl-benzimidazole bidentate ligands adorned with aliphatic chains. *Dalton Trans.* **53**, 14037–14045 (2024).
12. Halcrow, M. A. Mix and match - controlling the functionality of spin-crossover materials through solid solutions and molecular alloys. *Dalton Trans.* **53**, 13694–13708 (2024).
13. Molnár, G., Rat, S., Salmon, L., Nicolazzi, W. & Bousseksou, A. Spin crossover nanomaterials: from fundamental concepts to devices. *Adv. Mater.* **30**, 1–23 (2018).
14. Zhang, Y. et al. A molecular spin-crossover film allows for wavelength tuning of the resonance of a Fabry-Perot cavity. *J. Mater. Chem. C* **8**, 8007–8011 (2020).
15. Coronado, E. Molecular magnetism: from chemical design to spin control in molecules, materials and devices. *Nat. Rev. Mater.* **5**, 87–104 (2020).
16. Sun, L., Rotaru, A. & Garcia, Y. A non-porous Fe(II) complex for the colorimetric detection of hazardous gases and the monitoring of meat freshness. *J. Hazard. Mater.* **437**, 129364 (2022).
17. Ridier, K. et al. Unprecedented switching endurance affords for high-resolution surface temperature mapping using a spin-crossover film. *Nat. Commun.* **11**, 3611 (2020).
18. Zan, Y. et al. Soft actuators based on spin-crossover particles embedded in thermoplastic polyurethane. *Adv. Intell. Syst.* **5**, 2200432 (2023).
19. Harvey, J. N. Understanding the kinetics of spin-forbidden chemical reactions. *Phys. Chem. Chem. Phys.* **9**, 331–343 (2007).
20. Bhandary, S. et al. Manipulation of spin state of iron porphyrin by chemisorption on magnetic substrates. *Phys. Rev. B* **88**, 1–9 (2013).
21. Lomont, J. P., Nguyen, S. C. & Harris, C. B. Ultrafast infrared studies of the role of spin states in organometallic reaction dynamics. *Acc. Chem. Res.* **47**, 1634–1642 (2014).
22. Shankar, S. et al. Light-controlled switching of the spin state of iron(III). *Nat. Commun.* **9**, 4750 (2018).
23. Takayanagi, T. & Nakatomi, T. Automated reaction path searches for spin-forbidden reactions. *J. Comput. Chem.* **39**, 1319–1326 (2018).
24. Makris, T. M., von Koenig, K., Schlichting, I. & Sligar, S. G. Alteration of P450 distal pocket solvent leads to impaired proton delivery and changes in heme geometry. *Biochemistry* **46**, 14129–14140 (2007).

25. Pardo, A. et al. Density functional study of the catalytic cycle of nickel-iron [NiFe] hydrogenases and the involvement of high-spin nickel(II). *J. Biol. Inorg. Chem.* **11**, 286–306 (2006).
26. Harvey, J. N., Poli, R. & Smith, K. M. Understanding the reactivity of transition metal complexes involving multiple spin states. *Coord. Chem. Rev.* **238–239**, 347–361 (2003).
27. Halcrow, M. A. Manipulating metal spin states for biomimetic, catalytic and molecular materials chemistry. *Dalton Trans.* **49**, 15560–15567 (2020).
28. Swart, M. & Costas, M. (eds) *Spin States in Biochemistry and Inorganic Chemistry: Influence on Structure and Reactivity* (John Wiley & Sons, Ltd, Oxford, UK, 2015).
29. He, P. & Zhu, S. F. Spin crossover and its application in organometallic catalysis: concepts and recent progress. *Chemistry* https://doi.org/10.1002/chem.202403437 (2024).
30. Guengerich, F. P. Mechanisms of cytochrome P450-catalyzed oxidations. *ACS Catal.* **8**, 10964–10976 (2018).
31. Kalita, S., Shaik, S., Kisan, H. K. & Dubey, K. D. A paradigm shift in the catalytic cycle of P450: the preparatory choreography during O2 binding and origins of the necessity for two protonation pathways. *ACS Catal.* **10**, 11481–11492 (2020).
32. Surawatanawong, P., Tye, J. W. & Hall, M. B. Density functional theory applied to a difference in pathways taken by the enzymes cytochrome P450 and superoxide reductase: spin states of ferric hydroperoxo intermediates and hydrogen bonds from water. *Inorg. Chem.* **49**, 188–198 (2010).
33. Sheng, Y. et al. Superoxide dismutases and superoxide reductases. *Chem. Rev.* **114**, 3854–3918 (2014).
34. Stepanović, S., Angelone, D., Gruden, M. & Swart, M. The role of spin states in the catalytic mechanism of the intra- and extradiol cleavage of catechols by O2. *Org. Biomol. Chem.* **15**, 7860–7868 (2017).
35. Ray, K., Pfaff, F. F., Wang, B. & Nam, W. Status of reactive non-heme metal-oxygen intermediates in chemical and enzymatic reactions. *J. Am. Chem. Soc.* **136**, 13942–13958 (2014).
36. Buchachenko, A. L. & Berdinskii, V. L. Spin catalysis: dynamics of three-spin systems. *Russ. Chem. Bull.* **44**, 1578–1584 (1995).
37. Buchachenko, A. L. & Berdinsky, V. L. Spin catalysis of chemical reactions. *J. Phys. Chem.* **100**, 18292–18299 (1996).
38. Minaev, B. F. & Ågren, H. Spin-catalysis phenomena. *Int. J. Quantum Chem.* **57**, 519–532 (1996).
39. Takayanagi, T., Saito, K., Suziki, H., Watabe, Y. & Fujihara, T. Computational analysis of two-state reactivity in β-hydride elimination mechanisms of Fe(II)- and Co(II)-alkyl complexes supported by β-diketiminate ligand. *Organometallics* **38**, 3582–3589 (2019).
40. Bellows, S. M., Cundari, T. R. & Holland, P. L. Spin crossover during β-hydride elimination in high-spin iron(II)- and cobalt(II)-alkyl complexes. *Organometallics* **32**, 4741–4751 (2013).
41. Lee, W., Zhou, J. & Gutierrez, O. Mechanism of Nakamura's bisphosphine-iron-catalyzed asymmetric C(Sp2)-C(Sp3) cross-coupling reaction: the role of spin in controlling arylation pathways. *J. Am. Chem. Soc.* **139**, 16126–16133 (2017).
42. Sun, Y. et al. Two-state reactivity in low-valent iron-mediated C-H activation and the implications for other first-row transition metals. *J. Am. Chem. Soc.* **138**, 3715–3730 (2016).
43. Lutz, S. A., Hickey, A. K., Gao, Y., Chen, C. H. & Smith, J. M. Two-state reactivity in iron-catalyzed alkene isomerization confers σ-base resistance. *J. Am. Chem. Soc.* **142**, 15527–15535 (2020).
44. Macaulay, C. M. et al. Alkene isomerization-hydroboration catalyzed by first-row transition-metal (Mn, Fe, Co, and Ni) N-phosphinoamidinate complexes: origin of reactivity and selectivity. *ACS Catal.* **8**, 9907–9925 (2018).
45. Beromi, M. M., Younker, J. M., Zhong, H., Pabst, T. P. & Chirik, P. J. Catalyst design principles enabling intermolecular alkene-diene [2+2] cycloaddition and depolymerization reactions. *J. Am. Chem. Soc.* **143**, 17793–17805 (2021).
46. Cramer, H. H. et al. Ligand field sensitive spin acceleration in the iron-catalyzed [2 + 2] cycloaddition of unactivated alkenes and dienes. *J. Am. Chem. Soc.* **146**, 9947–9956 (2024).
47. He, P. et al. Spin effect on redox acceleration and regioselectivity in Fe-catalyzed alkyne hydrosilylation. *Natl. Sci. Rev*. https://doi.org/10.1093/nsr/nwad324 (2024).
48. He, P. et al. Iron-catalyzed allylic C(Sp3)−H silylation: spin-crossover-efficiency-determined chemoselectivity. *Angew. Chemie Int. Ed.* **63**, 1–9 (2024).
49. Wang, Q. et al. Precise regulation of iron spin states in single Fe-N4 sites for efficient peroxidase-mimicking catalysis. *Small* **18**, 1–7 (2022).
50. Mizrahi, A. et al. Electronic coupling and electrocatalysis in redox active fused iron corroles. *Inorg. Chem.* **61**, 20725–20733 (2022).
51. Yu, M., Li, A., Kan, E. & Zhan, C. Substantial impact of spin state evolution in OER/ORR catalyzed by Fe-N-C. *ACS Catal.* **14**, 6816–6826 (2024).
52. Yu, M. et al. Strain-controlled spin regulation in Fe-N-C catalysts for enhanced oxygen reduction reaction activity. *J. Mater. Chem. A* **12**, 24530–24541 (2024).
53. Wang, Y. et al. Regulation of atomic Fe-spin state by crystal field and magnetic field for enhanced oxygen electrocatalysis in rechargeable zinc-air batteries. *Angew. Chemie Int. Ed*. https://doi.org/10.1002/anie.202304229 (2023).
54. Du, Z. et al. Rapid surface reconstruction of pentlandite by high-spin state iron for efficient oxygen evolution reaction. *Angew. Chemie Int. Ed*. https://doi.org/10.1002/anie.202317022 (2024).
55. Wang, C.-F., Yang, G.-Y., Yao, Z.-S. & Tao, J. Monitoring the spin states of ferrous ions by fluorescence spectroscopy in spin-crossover–fluorescent hybrid materials. *Chem. Eur. J.* **24**, 3218–3224 (2018).
56. Getzner, L. et al. Combining electron transfer, spin crossover, and redox properties in metal-organic frameworks. *Nat. Commun*. https://doi.org/10.1038/s41467-024-51385-8 (2024).
57. Lyu, B.-H. et al. Successive redox modulation in an iron(<scp>ii</Scp>) spin-crossover framework. *Inorg. Chem. Front.* **10**, 3577–3583 (2023).
58. Martinez-Martinez, A. et al. Spin crossover-assisted modulation of electron transport in a single-crystal 3D metal-organic framework. *Chem. Mater.* **35**, 6012–6023 (2023).
59. Wu, S. G. et al. Redox-programmable spin-crossover behaviors in a cationic framework. *J. Am. Chem. Soc.* **144**, 14888–14896 (2022).
60. Gong, Y.-N. et al. Regulating photocatalysis by spin-state manipulation of cobalt in covalent organic frameworks. *J. Am. Chem. Soc.* **142**, 16723–16731 (2020).
61. Palacios-Corella, M. et al. Redox and guest tunable spin-crossover properties in a polymeric polyoxometalate. *Chem. Sci.* **14**, 3048–3055 (2023).
62. Wu, D. et al. Spin manipulation in a metal–organic layer through mechanical exfoliation for highly selective CO2 photoreduction. *Angew. Chemie Int. Ed*. https://doi.org/10.1002/anie.202301925 (2023).
63. Zhang, J., Kosaka, W., Kitagawa, Y. & Miyasaka, H. A host–guest electron transfer mechanism for magnetic and electronic modifications in a redox-active metal–organic framework. *Angew. Chemie Int. Ed.* **61**, 1–9 (2022).
64. Huang, G.-Z. et al. On–off switching of a photocatalytic overall reaction through dynamic spin-state transition in a Hofmann Clathrate system. *J. Am. Chem. Soc.* **145**, 26863–26870 (2023).
65. Wang, H. Y. et al. Photo- and electronically switchable spin-crossover iron(II) metal–organic frameworks based on a tetrathiafulvalene ligand. *Angew. Chemie Int. Ed.* **56**, 5465–5470 (2017).
66. Umeyama, D., Takai, A. & Sonobe, K. Postsynthetic defect formation in three-dimensional Hofmann-type coordination polymers and its impact on catalytic activity. *Inorg. Chem.* **61**, 1697–1703 (2022).

67. Wang, Z. & Cohen, S. M. Postsynthetic covalent modification of a neutral metal-organic framework. *J. Am. Chem. Soc.* **129**, 12368–12369 (2007).
68. Walsh, C. T., Garneau-Tsodikova, S. & Gatto, G. J. Protein posttranslational modifications: the chemistry of proteome diversifications. *Angew. Chemie Int. Ed.* **44**, 7342–7372 (2005).
69. Enríquez-Cabrera, A., Ridier, K., Salmon, L., Routaboul, L. & Bousseksou, A. Complete and versatile post-synthetic modification on iron-triazole spin crossover complexes: a relevant material elaboration method. *Eur. J. Inorg. Chem.* **2021**, 2000–2016 (2021).
70. Wang, C. F. et al. Synergetic spin crossover and fluorescence in one-dimensional hybrid complexes. *Angew. Chemie Int. Ed.* **54**, 1574–1577 (2015).
71. Askew, J. H. & Shepherd, H. J. Post-synthetic anion exchange in iron(Ii) 1,2,4-triazole based spin crossover materials: via mechanochemistry. *Dalton Trans.* **49**, 2966–2971 (2020).
72. Resines-Urien, E. et al. Covalent post-synthetic modification of switchable iron-based coordination polymers by volatile organic compounds: a versatile strategy for selective sensor development. *Dalton Trans.* **49**, 7315–7318 (2020).
73. Enríquez-Cabrera, A., Routaboul, L., Salmon, L. & Bousseksou, A. Complete post-synthetic modification of a spin crossover complex. *Dalton Trans.* **48**, 16853–16856 (2019).
74. Enríquez-Cabrera, A., Getzner, L., Salmon, L., Routaboul, L. & Bousseksou, A. Post-synthetic modification mechanism for 1D spin crossover coordination polymers. *New J. Chem.* **46**, 22004–22012 (2022).
75. Gural'skiy, I. A., Shylin, S. I., Ksenofontov, V. & Tremel, W. Spin-state-dependent redox-catalytic activity of a switchable iron(II) complex. *Eur. J. Inorg. Chem.* **2017**, 3125–3131 (2017).
76. Bell-Taylor, A., Gorden, J. D., Hardy, E. E. & Goldsmith, C. R. A spin-crossover Co(II) complex catalyzes the activation of Sp3 C–H bonds by two-electron oxidants. *Inorg. Chim. Acta* **482**, 206–212 (2018).
77. Higuchi, M., Hitomi, Y., Minami, H., Tanaka, T. & Funabiki, T. Correlation of spin states and spin delocalization with the dioxygen reactivity of catecholatoiron(III) complexes. *Inorg. Chem.* **44**, 8810–8821 (2005).
78. Prat, I. et al. Assessing the impact of electronic and steric tuning of the ligand in the spin state and catalytic oxidation ability of the feii(pytacn) family of complexes. *Inorg. Chem.* **52**, 9229–9244 (2013).
79. Zoumpanioti, M. et al. Esterification reactions catalyzed by lipases immobilized in organogels: effect of temperature and substrate diffusion. *Biotechnol. Lett.* **30**, 1627–1631 (2008).
80. Fenske, T., Korth, H.-G., Mohr, A. & Schmuck, C. Advances in switchable supramolecular nanoassemblies. *Chem. Eur. J.* **18**, 738–755 (2012).
81. Treat, N. D., Mates, T. E., Hawker, C. J., Kramer, E. J. & Chabinyc, M. L. Temperature dependence of the diffusion coefficient of PCBM in poly(3-hexylthiophene). *Macromolecules* **46**, 1002–1007 (2013).
82. Subba, N. et al. Temperature-dependent ultrafast solvation response and solute diffusion in acetamide-urea deep eutectic solvent. *J. Phys. Chem. B* **123**, 9212–9221 (2019).
83. Knopf, D. A. & Ammann, M. Technical note: Adsorption and desorption equilibria from statistical thermodynamics and rates from transition state theory. *Atmos. Chem. Phys.* **21**, 15725–15753 (2021).
84. Khamis, F., Hegab, H. M., Banat, F., Arafat, H. A. & Hasan, S. W. Comprehensive review on PH and temperature-responsive polymeric adsorbents: mechanisms, equilibrium, kinetics, and thermodynamics of adsorption processes for heavy metals and organic dyes. *Chemosphere* **349**, 140801 (2024).
85. Nesterkina, M., Kravchenko, I., Hirsch, A. K. H. & Lehr, C. M. Thermotropic liquid crystals in drug delivery: a versatile carrier for controlled release. *Eur. J. Pharm. Biopharm.* **200**, 114343 (2024).
86. Walton, R. I. Subcritical solvothermal synthesis of condensed inorganic materials. *Chem. Soc. Rev.* **31**, 230–238 (2002).
87. Gholami, T. et al. A review on investigating the effect of solvent on the synthesis, morphology, shape and size of nanostructures. *Mater. Sci. Eng. B* **304**, 117370 (2024).
88. Demazeau, G. Solvothermal processes: a route to the stabilization of new material. *J. Mater. Chem.* **9**, 15–18 (1999).
89. Grosjean, A. et al. Crystal structures and spin crossover in the polymeric material [Fe(Htrz) 2 (Trz)](BF 4) including coherent-domain size reduction effects. *Eur. J. Inorg. Chem.* **2013**, 796–802 (2013).
90. Grosjean, A. et al. Crystallinity and microstructural versatility in the spin-crossover polymeric material [Fe(Htrz) 2 (Trz)](BF 4). *Eur. J. Inorg. Chem.* **2018**, 429–434 (2018).
91. Grosjean, A. et al. The spin-crossover phenomenon at the coherent-domains scale in 1D polymeric powders: evidence for structural fatigability. *Eur. J. Inorg. Chem.* **2016**, 1961–1966 (2016).
92. Grosjean, A. *Matériaux polymériques 1D à Transition de Spin: Investigations Structurales Multi-Échelles* (Université de Bordeaux 1, 2013).
93. Grosjean, A. et al. The 1-D polymeric structure of the [Fe(NH 2trz) 3] (NO 3) 2·nH 2O (with n = 2) spin crossover compound proven by single crystal investigations. *Chem. Commun.* **47**, 12382–12384 (2011).
94. Yang, X. et al. Room temperature spin crossover properties in a series of mixed-anion Fe(NH2trz)3(BF4)2−x(SiF6)x/2 complexes. *Dalton Trans*. https://doi.org/10.1039/d4dt00267a (2024).
95. Paliwoda, D. et al. Elastic properties of the iron(II)–triazole spin crossover complexes [Fe(Htrz) 2 Trz]BF 4 and [Fe(NH2 Trz) 3]SO4. *Cryst. Growth Des.* **23**, 1903–1914 (2023).

Acknowledgements

We are thankful for financial support from the Agence Nationale de la Recherche (ANR-19-CE09-0008-01), the A.E.C. thanks the CONACyT (Mexico) and the ANR for postdoctoral grants, and Y.L. thanks the China Scholarship Council for a PhD grant. We would like to thank our research group, especially Livia and Gábor for helping us improve the quality of the writing in English.

Author contributions

Y.L. (experimental work), A.E.C. (experimental work, manuscript), L.S. & A.B. (manuscript), L.R. (manuscript, conceptualization, and supervised the project).

Competing interests

The authors declare no competing interests.

Additional information

Supplementary information The online version contains supplementary material available at https://doi.org/10.1038/s42004-025-01425-1.

Correspondence and requests for materials should be addressed to Lionel Salmon, Lucie Routaboul or Azzedine Bousseksou.

Peer review information *Communications Chemistry* thanks the anonymous reviewers for their contribution to the peer review of this work. Peer review reports are available.